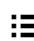
 About  Sections



Advei

STEM CELLS / Volume 33, Issue 4

Tissue-Specific Stem Cells | 

## Human White and Brite Adipogenesis is Supported by MSCA1 and is Impaired b Immune Cells

David Estève, Nathalie Boulet, Fanny Volat, Alexia Zakaroff-Girard, Séverine Ledoux, Muriel Coupaye, Pauline Decaunes, Chloé Belles, Frederique Gaits-Iacovoni, Jason S. Iacovoni, ... [See all authors](#) ▾

First published: 18 December 2014

<https://doi.org/10.1002/stem.1916>

Cited by:12

### Abstract

Obesity-associated inflammation contributes to the development of metabolic diseases. Although brite adipocytes have been shown to ameliorate metabolic parameters in rodents, their origin and differentiation remain to be characterized in humans. Native CD45<sup>-</sup>/CD34<sup>+</sup>/CD31<sup>-</sup> cells have been previously described as human adipocyte progenitors. Using two additional cell surface markers, MSCA1 (tissue nonspecific alkaline phosphatase) and CD271 (nerve growth factor receptor), we are able to partition the CD45<sup>-</sup>/CD34<sup>+</sup>/CD31<sup>-</sup> cell population into three subsets. We establish serum-free culture conditions without cell expansion to promote either white/brite adipogenesis using rosiglitazone, or bone morphogenetic protein 7 (BMP7), or specifically brite adipogenesis using 3-isobutyl-1-methylxanthine. We demonstrate that adipogenesis leads to an increase of MSCA1 activity, expression of white/brite adipocyte-related genes, and mitochondriogenesis. Using pharmacological inhibition and gene silencing approaches, we show that MSCA1 activity is required for triglyceride accumulation and for the expression of white/brite-related genes in human cells. Moreover, native immunoselected MSCA1<sup>+</sup> cells exhibit brite precursor characteristics and the highest adipogenic potential of the three progenitor subsets. Finally, we provided evidence that MSCA1<sup>+</sup> white/brite precursors accumulate with obesity in subcutaneous adipose tissue (sAT), and that local BMP7 and



About Sections

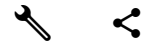


## Introduction

While obesity in humans is associated with a low-grade inflammatory state and an increased risk to develop cardiovascular and metabolic pathologies, the link between excessive adipose tissue (AT) and metabolic abnormalities remains to be clearly defined. In the last decade, two concepts have emerged. The first concept is related to AT expandability and its buffering activity toward toxic free fatty acids. First of all, AT expandability depends on a physiological turnover of adipocytes, hyperplasia, the formation of new adipocytes from progenitors, and hypertrophy, the capacity of mature adipocytes to increase triglyceride storage. Hyperplasia and adipocyte turnover are sustained by an active, multistep process called adipogenesis. A defect in adipogenesis at the level of adipogenic commitment of mesenchymal stem/progenitor cells to become preadipocytes and/or at the level of preadipocyte differentiation into adipocytes could limit AT expandability and therefore promote insulin resistance [1](#). The second concept involves a new type of adipocyte referred to as the brite adipocyte which ameliorated insulin resistance status in rodent [2](#). Brite, also called beige, adipocytes share some common features with brown adipocytes, such as the expression of mitochondrial uncoupling protein 1 (UCP1) and a high mitochondrial content, despite the fact that they reside in white fat depots, predominantly in subcutaneous AT (sAT) [2-4](#). While PPAR agonists have been known to ameliorate insulin sensitivity and promote adipogenesis, they have only recently been shown to promote the appearance of brite adipocytes in mice cells and white AT [5-7](#). In addition, other stimuli such as  $\beta$ -adrenergic receptor agonists or members of the bone morphogenetic protein (BMP) family have been described to favor the appearance of brite adipocytes in rodent sAT [8-10](#). Using in vivo cell tracking approaches, murine brite adipocytes have been shown to arise either from the conversion of mature white adipocytes or from the differentiation of AT progenitor cells [11, 12](#), described as positive for PDGFR $\alpha$  as well as TMEM26, CD137, and CD40 [4, 13](#). In humans, the existence of a brite adipocyte phenotype in situ remains to be clearly demonstrated, although the expression of brite precursor-related genes was observed in supraclavicular locations [14, 15](#). We showed, in vitro that native CD45 $^-$ /CD34 $^+$ /CD31 $^-$  progenitor cells from adult human AT supported both white and brite adipogenic potentials under PPAR $\gamma$  agonist treatment [16, 17](#). To further discriminate between the specific white and brite precursor cells within the CD45 $^-$ /CD34 $^+$ /CD31 $^-$  progenitor cells, we investigated additional mesenchymal cell surface markers, both in situ and in vitro. We focused on MSCA1, the tissue nonspecific alkaline phosphatase (AP) [18](#) and on



About Sections



conditions without cell expansion to avoid confounding effect of cell proliferation in order to identify human white and brite adipogenic precursors. We developed immunoselection/depletion approaches to partition native progenitor cells into three distinct subsets: CD271+/MSCA1+ (Msca1+), CD271+/MSCA1- (-/Cd271+), and CD271-/MSCA1- (-/-). We provide evidence that MSCA1 is a functional marker of human white and brite adipogenic precursor cells. Therefore, we suggest that in adult human AT, the native progenitor cells are composed of subsets in distinct stages of adipogenic process, the Msca1+ cell subset being the most committed cells toward white and brite adipogenesis. We hypothesize that the accumulation of Msca1+ cells in obese AT might reflect a defect in the last stage of white/brite adipocyte differentiation, due to immune cell accumulation.

## Methods

### Adipose Tissue Collection

Cohort 1: Subcutaneous human AT were obtained from healthy adult women undergoing aesthetic plastic surgery ( $n = 59$ , mean Body mass index (BMI)  $28 \pm 5.6$  kg/m<sup>2</sup> (21.3–39.3), mean age  $43.1 \pm 11.9$  years (26–69)). Cohort 2: Subcutaneous AT were obtained from nonobese women undergoing gynecological surgery (Supporting Information Table 1). sAT and viscera AT (vAT) matched biopsies were obtained from morbidly obese patients undergoing gastric bypass surgery (Supporting Information Table 2) ([ClinicalTrials.gov](https://clinicaltrials.gov/ct2/show/study/NCT01525472) Identifier: NCT01525472). All donors gave their informed consent.

### Isolation of AT Stroma-Vascular Cells

AT was digested with dispase (2.4 U/ml in phosphate-buffered saline (PBS), pH 7.4, v/v) then collagenase (250 U/ml in PBS, 2% bovine serum albumin (BSA), pH 7.4, v/v) for 30 minutes at 37°C, the cell suspension was filtered with a 250- $\mu$ m filter. The stroma-vascular cells (SVC) were obtained after centrifugation (room temperature) and treatment with erythrocyte lysis buffer (155 mmol/L NH<sub>4</sub>Cl; 5.7 mmol/L K<sub>2</sub>HPO<sub>4</sub>; 0.1 mmol/L EDTA; pH 7.3) for 10 minutes. Finally, matrix fragments were removed using successive filtrations through 100, 70, and 40  $\mu$ m nylon meshes.

SVC were plated at high density (120,000 cells per cm<sup>2</sup>) for 48 hours in Endothelial cell growth medium-microvascular vessels (ECGM-MV) (Promocell) or at low density (30,000 cells per cm<sup>2</sup>) until high density. Cells were then analyzed for cell surface markers by flow cytometry.



About Sections



Technologies, Vancouver, BC, Canada, <http://www.stemcell.com>) followed by an endothelial cell depletion step using an anti-CD31-depletion kit (R&D Systems Minneapolis, MN, <http://www.rndsystems.com>) following each manufacturer's protocol. To further isolate the distinct progenitor cell subsets, the MSCA1<sup>+</sup> cells were selected from the CD45<sup>-</sup>/CD31<sup>-</sup> cells, the <sup>-</sup>/CD271<sup>+</sup> cells were selected from the CD45<sup>-</sup>/CD31<sup>-</sup>/MSCA1<sup>-</sup> cells, and the CD45<sup>-</sup>/CD31<sup>-</sup>/MSCA1<sup>-</sup>/CD271<sup>-</sup> (-/-) cells using CD34 immunomagnetic selection kits to improve the purity of this cell subset (MSCA1<sup>+</sup>, CD271<sup>+</sup>, and CD34<sup>+</sup> immunomagnetic selection kits were from Miltenyi Biotec, Bergisch Gladbach, Germany, <http://www.miltenyibiotec.com>). The purity of each fraction was assessed by flow cytometry analyses. Lymphocytes and macrophages were sorted as previously described [21](#).

## Flow Cytometry Analyses

Cells were incubated with fluorescent-labeled monoclonal antibodies or their respective controls (30 minutes, 4°C) (anti-human CD45 V500-conjugated, CD34 Peridinin chlorophyll (PerCP)-conjugated, CD31 V450-conjugated, from BD Biosciences, San Diego, CA, <http://www.bdbiosciences.com>; anti-human MSCA1 R-Phycoerythrin (PE)-conjugated and CD271 Allophycocyanin (APC)-conjugated, from Miltenyi Biotec). Intracellular stainings for IFN- $\gamma$  were performed using PE-CY7 conjugated antibody (BD Biosciences) and BD cytofix/cytoperm reagent (BD Biosciences) Mitochondrial content was assessed using Mitotracker green FM (2 nmol/L, Life Technologies, Rockville, MD, <http://www.lifetech.com>) for 30 minutes at 37°C before cell surface staining. After washing steps, the cells were analyzed by flow cytometry using a FACS Canto II flow cytometer and Diva Pro software (BD Biosciences).

## Adipogenic Culture Conditions

Cells (SVCs, isolated progenitor cells or progenitor cell subsets) were plated at high density (120,000 cells per cm<sup>2</sup>). 36 to 48 hours after seeding, medium was changed into basal defined adipogenic medium: ECBM (Promocell), 50 mg/mL penicillin-streptomycin, 66 nmol/L insulin, 66 nmol/L triiodothyronine, 0.1  $\mu$ g/mL transferrin, 100 nmol/L cortisol (ITTC) supplemented or not with 3  $\mu$ M Rosiglitazone (ITTCR) or 0.25 mM isobuthylmethylxanthine (IBMX) (ITTCX). After 3 days, the media was replaced with basal defined adipogenic medium and refreshed every 2 days for the following 7 days. For BMP7 treatment, progenitor cells were plated in growth medium supplemented or not with 50 ng/mL of human recombinant BMP7 (PeproTech, Rock Hill, NJ, <http://www.peprotech.com>) for 2 days. Progenitor cells were cultured with basal



About Sections



cells were cultured in adipogenic media containing rosiglitazone (described above) supplemented or not with 10 ng/mL of tumor necrosis factor (TNF $\alpha$ ), interferon (IFN $\gamma$ ), or interleukin (IL) 17 (PeproTech, Rocky Hill, NJ, <http://www.peprotech.com>

## mRNA Extraction and Real-Time Polymerase Chain Reaction

Total RNAs were extracted using the RNeasy kit (Qiagen, Hilden, Germany, <http://www1.qiagen.com>). The RNA concentration was measured with Ribogreen (Invitrogen Carlsbad, CA, <http://www.invitrogen.com>). RNAs were reverse-transcribed using Superscript kit (Invitrogen). TaqMan Primers are listed in Supporting Information Table 3. The amplification reaction was done on 15 ng of the cDNA samples in a final volume of 20  $\mu$ L in 96-well reaction plates in a GeneAmp 7500 detection system and software (Applied Biosystems, Foster City, CA, <http://www.appliedbiosystems.com>). Results were normalized to 18S rRNA levels.

## Western Blot

Cells were lysed with RIPA buffer, protein content was determined by bicinchoninic acid (BCA) assay (Pierce, Rockford, IL, <http://www.piercenet.com>). Proteins were loaded on 4%–12% BisTris electrophoresis gel. Nitrocellulose membrane was incubated with antibodies (UCP1 (Sigma-Aldrich), OXPHOS (Abcam, Cambridge, U.K., <http://www.abcam.com>), SMAD1, P-SMAD1/5/8, ERK1/2, P-ERK1/2, P38MAPK, P-P38MAPK,  $\beta$ -actin (Cell Signaling Technology, Beverly, MA, <http://www.cellsignal.com>), BMP7 (Abcam)) overnight at 4°C in Tris Borate Sodium buffer containing 5% BSA or 5% milk. Horseradish peroxidase (HRP) secondary antibody (Cell Signaling Technology) was incubated 1 hour at room temperature (RT). Peroxidase activity was evaluated using West Dura reagent (Pierce, Rockford, IL, <http://www.piercenet.com>) and the Chemidoc detection system (Bio-Rad Laboratories, Hercules, CA, <http://www.bio-rad.com>).

## Immunofluorescence Staining

Cells or AT were fixed with paraformaldehyde 4% at RT for 10 minutes (cultured cells) or up to 1 hour (AT). Samples were incubated for 15 minutes with BODIPY 493/503 (10  $\mu$ g/mL, Invitrogen) or with primary antibody (UCP1, (Sigma-Aldrich), anti-mitochondria MAB1273 (Clone 113-1, Millipore, Billerica, MA, <http://www.millipore.com>), CD271 (Clone ME20.4, Santa Cruz Biotechnology, Santa Cruz, CA, <http://www.scbt.com>), MSCA1 (Clone W8B2, Miltenyi Biotec) and CD34 (clone EP373Y, Epitomics)) for 1 hour at RT (overnight at 4°C for AT). Then samples were incubated with appropriate secondary antibodies coupled with Alexa Fluor 488



About Sections



## Alkaline Phosphatase Activity

Cells were lysed with Tris (0.1 mM), NaCl (155 mM), 0.1% Triton X-100. Cell lysates were incubated at 37°C with 50 μM of 4-methylumbelliferyl-phosphate (MUP, Sigma-Aldrich) in appropriate buffer. Kinetics of MUP degradation was assessed by fluorescence every 3 minutes during 60 minutes and normalized by protein content.

## MSCA1 Inhibition by endoribonuclease-prepared siRNAs (esiRNA)

Progenitor cells were seeded at a density of 90,000 cells per cm<sup>2</sup>. Cells were transfected with 500 ng/mL of MISSION esiRNA (Sigma-Aldrich) against MSCA1 or green fluorescent protein (GFP) as negative control with 1 μL of lipofectamine 2000 (Invitrogen) in 1 mL of ECBM (Promocell). After 12 hours, medium was removed and cells were cultured under adipogenic conditions (ITTCR).

## Statistical Analyses

Statistical analyses were performed using Prism (GraphPad Software). Comparisons between groups were analyzed either by two-tailed paired Student's *t* test or one-way ANOVA followed by Bonferroni post-tests for (*n*) independent experiments. Correlations were obtained using Spearman test. Differences were considered statistically significant when  $p < .05$ .

## Results

### CD45<sup>-</sup>/CD34<sup>+</sup>/CD31<sup>-</sup> Progenitor Cells are a Heterogeneous Cell Population

Multiparameter flow cytometry analyses were performed on native SVC from subcutaneous abdominal AT (sAT) from cohort 1 (See Materials and Methods section) using anti-CD45, -CD31, -CD271, and -MSCA1 antibodies. Three cell subsets were identified in the gated CD45<sup>-</sup>/CD34<sup>+</sup>/CD31<sup>-</sup> progenitor cell population, referred to as Msca1<sup>+</sup> (CD45<sup>-</sup>/CD34<sup>+</sup>/CD31<sup>-</sup>/CD271<sup>+</sup>/MSCA1<sup>+</sup>), -/Cd271<sup>+</sup> (CD45<sup>-</sup>/CD34<sup>+</sup>/CD31<sup>-</sup>/CD271<sup>+</sup>/MSCA1<sup>-</sup>), and -/- (CD45<sup>-</sup>/CD34<sup>+</sup>/CD31<sup>-</sup>/CD271<sup>-</sup>/MSCA1<sup>-</sup>) (Fig. 1A). The Msca1<sup>+</sup> cell subset represented a minor cell subset within progenitor cells (Fig. 1A). When comparing sAT to matched vAT from morbidly obese women from cohort 2 (Supporting Information Table 2), Msca1<sup>+</sup> cell content was markedly higher in sAT compared to vAT (Fig. 1B). We examined the effect of in vitro expansion on cel



 About  Sections



CD271<sup>+</sup> immunoselected cells from native sAT (progenitor cells, endothelial cells, macrophages, and lymphocytes) and mature unilocular adipocytes from sAT showed that progenitor cells exhibited the highest gene expression of MSCA1 and CD271 (Fig. 1E). Immunohistochemistry analyses performed on whole AT revealed that mature adipocytes do not express CD271 and MSCA1. Cells positive for CD271 and MSCA1 were also CD34 positive and were located at both perivascular and stromal position (Supporting Information Fig. 1).



About Sections

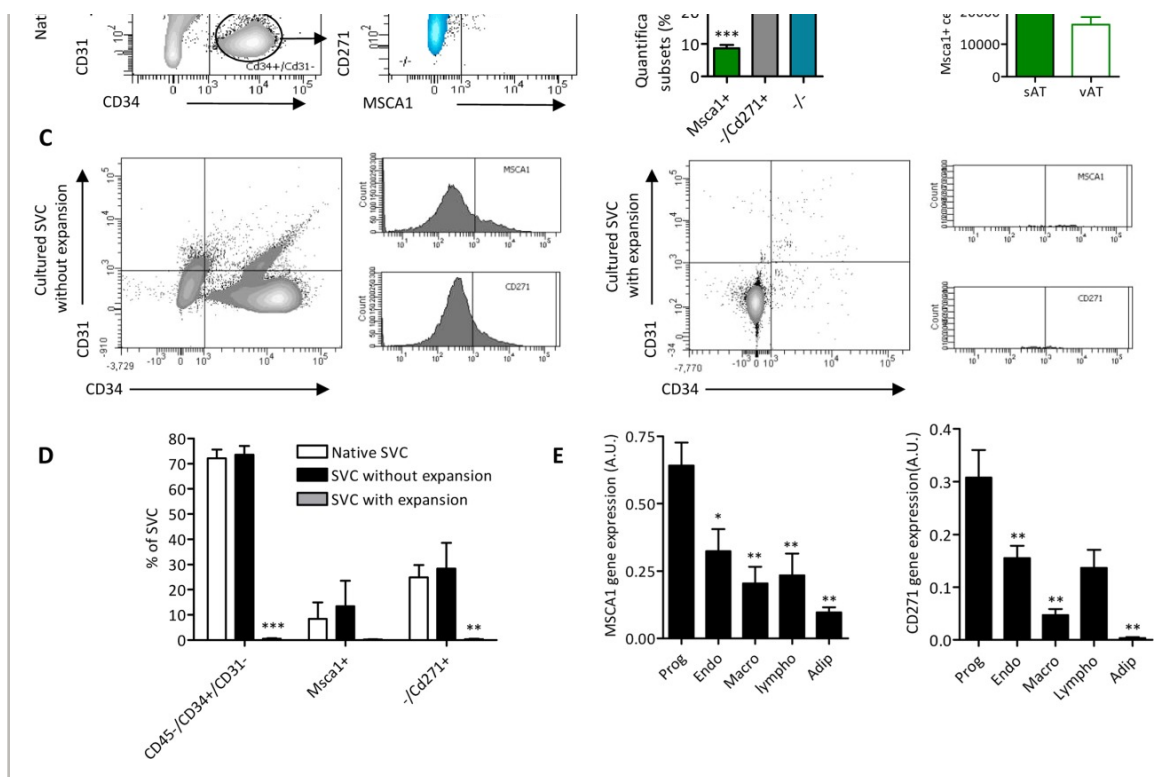


**Figure 1**

[Open in figure viewer](#) | [PowerPoint](#)

CD45-/CD34+/CD31- progenitor cell population is heterogeneous. **(A):** Representative dot-plots obtained by flow cytometry analyses with SVC from human sAT from cohort 1 using anti-CD31 and -CD34 antibodies (left) or anti-MSCA1 and -CD271 antibodies gated on CD45-/CD34+/CD31- cells (middle) and quantification of the CD45-/CD34+/CD31-/MSCA1+/CD271+ (MscA1+, green), CD45-/CD34+/CD31-/MSCA1-/CD271+ (-/Cd271+, grey), and CD45-/CD34+/CD31-/MSCA1-/CD271- (-/-, blue) cells (right) ( $n = 53$ , \*\*\*,  $p < .001$  vs. -/Cd271+ and -/- subset). **(B):** Quantification by flow cytometry of the number of MscA1+ cells per gram of AT from paired sAT and vAT from morbidly obese women (cohort 2,  $n = 72$ , \*\*\*,  $p < .001$ ). **(C):** Representative dot-plots obtained by flow cytometry using anti-CD31 and -CD34 antibodies and representative histograms using anti-MSCA1 and -CD271 antibodies gated on CD34+/CD31- cells with SVC seeded at high density and cultured 2 days (left) and SVC seeded at low density and cultured until high density (right). **(D):** Quantifications of CD45-/CD34+/CD31- progenitor cells, MscA1+ and





 About  Sections



adipogenic media (ITTC) supplemented with rosiglitazone for the 3 first days. The adipogenic induction shown by the time-dependent triglyceride accumulation (Fig. 2A; Supporting Information Fig. 2A) was associated with decreased CD271 expression (Fig. 2B) and marked increases in MSCA1 transcript levels and MSCA1-related AP activity (Fig. 2C). The expression of classic adipogenic-related genes (PPAR $\gamma$ 2, ChREBP, LPL, GPDH, and PLIN1) was markedly increased with adipogenesis (Fig. 2D) as well as the ones of brite adipocyte-related genes (UCP1, PGC1 $\alpha$ , CIDEA, CITED1, ELOVL3) (Fig. 2E). In parallel, the cell content in the mitochondrial OXPHOS proteins forming the respiratory chain evaluated by Western blot analyses increased and more particularly the complexes I, III, and IV (Fig. 2F). Further analysis of the mitochondrial architecture and UCP1 expression was performed at day 10 (Fig. 2G). Marked changes in mitochondrial network were observed in cells depending on the presence of lipid droplets, with a fused mitochondrial network in nonlipid-laden cells and a fissioned mitochondrial network in cells containing multiple lipid droplets. In such lipid-laden cells, 34  $\pm$  9% cells expressed UCP1 protein that colocalized with mitochondrial labeling. To note, two distinct UCP1 antibodies showed similar staining patterns (Supporting Information Fig. 2C).



About Sections

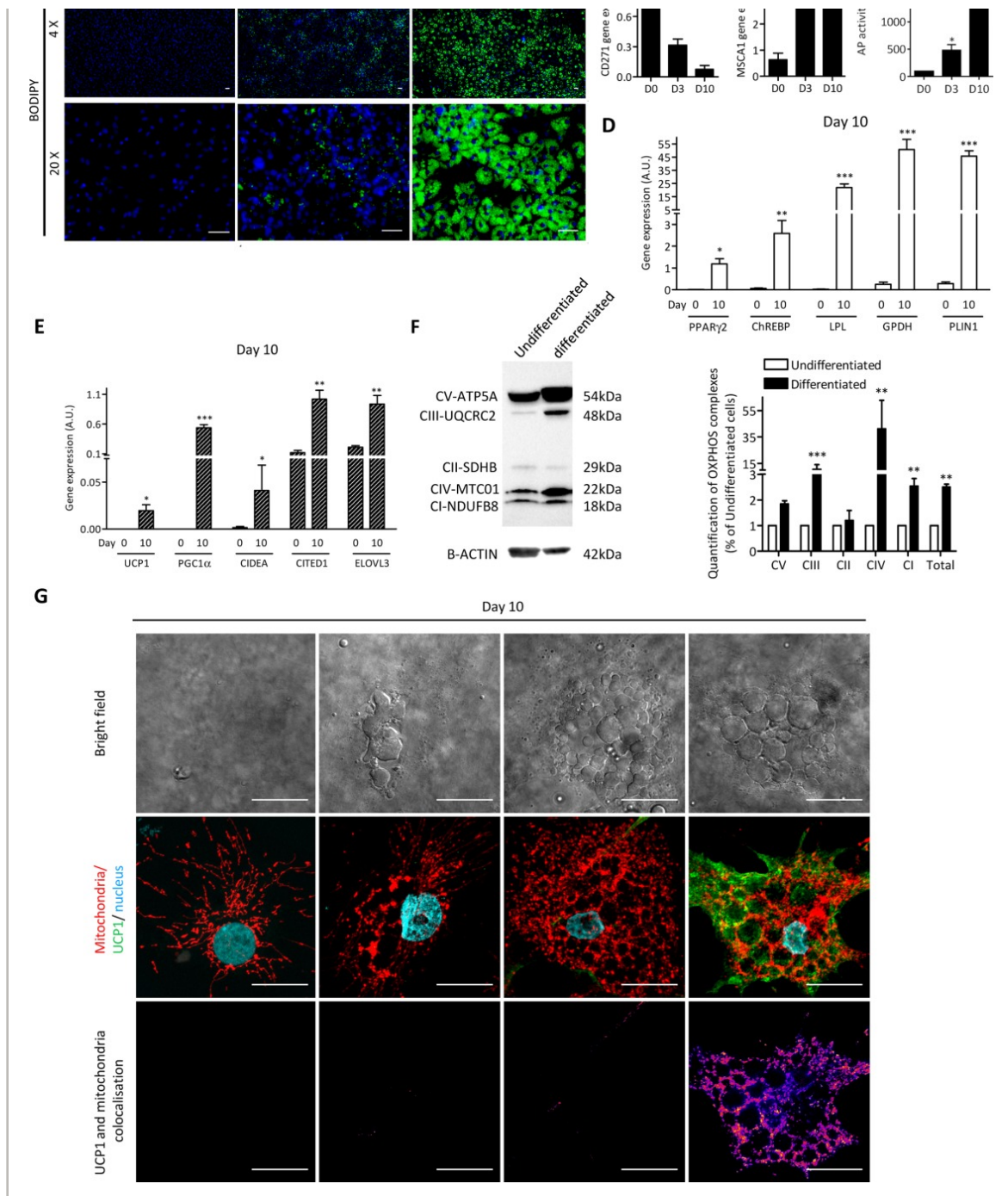


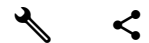
**Figure 2**

[Open in figure viewer](#) | [PowerPoint](#)

MSCA1 expression and activity increase with adipogenesis induced by rosiglitazone. CD45<sup>-</sup>/CD34<sup>+</sup>/CD31<sup>-</sup> progenitor cells were cultured under adipogenic conditions for 10 days with an initial 2 day treatment with



 About  Sections



13. To mimic this effect in vitro with human cells, we used the phosphodiesterase inhibitor IBMX, a classic cAMP-elevating compound. Cells plated at high density were cultured in three distinct serum-free adipogenic conditions: ITTC alone, ITTC supplemented with IBMX (ITTCX) or rosiglitazone (ITTCR) for the 3 first days (Fig. 3A). The extent of triglyceride accumulation (Fig. 3B; Supporting Information Fig. 2B) as well as MSCA1 expression and activity (Figure 3C) were found to be intermediate in ITTCX compared to ITTC and ITTCR conditions. The induction of classic adipogenic-related genes (PPAR $\gamma$ 2, GPDH, LPL, and PLIN1) was found similar in both ITTC and ITTCX conditions while markedly enhanced under ITTCR conditions except for ChREBP expression (Fig. 3D). Interestingly, the induction of brite-related genes (UCP1, CIDEA, CITED1, ELOVL3) was intermediate in ITTCX compared to ITTC and ITTCR (Fig. 3G). To note PGC1 $\alpha$  transcript levels did not follow such a pattern. The specific brite adipogenic induction mediated by IBMX was confirmed by UCP1 immunohistochemistry and Western blot analysis (Fig. 3E, 3F).



About Sections

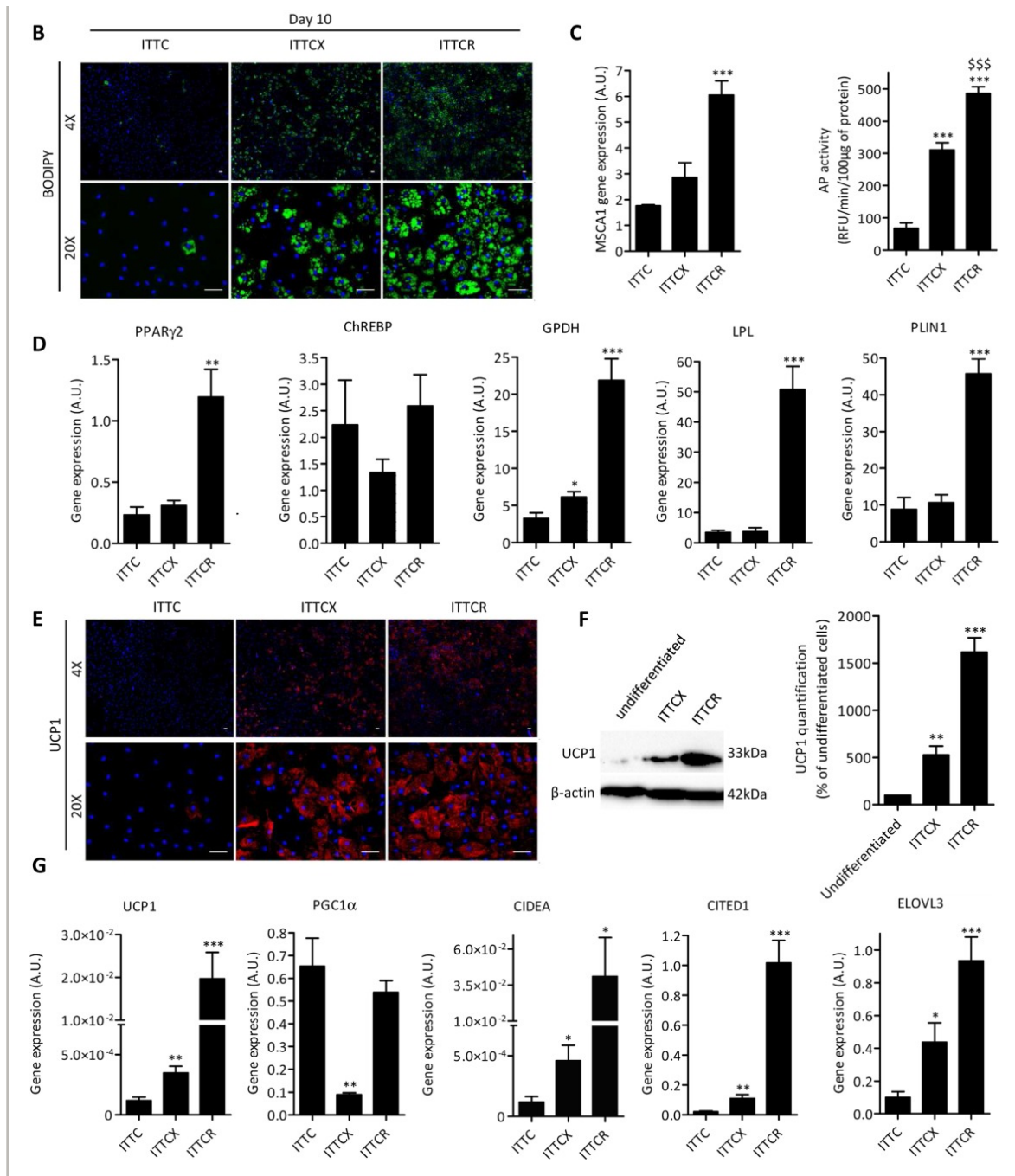


**Figure 3**

[Open in figure viewer](#) | [PowerPoint](#)

IBMX induces brite adipogenesis and increases MSCA1 expression and activity. **(A)**: CD45<sup>-</sup>/CD34<sup>+</sup>/CD31<sup>-</sup> progenitor cells were cultured under basal adipogenic condition (ITTC) for 10 days with an initial 3 day treatment in ITTC



 About  Sections



white and brite adipogenesis and its physiological relevance in AT. BMP7 transcript levels were detected predominantly in progenitor cells when compared to other AT-cell populations, that is, mature adipocytes, endothelial cells, and immune cells (Fig. 4A). Western blotting of progenitor cells identified a BMP7 propeptide at 49 kDa (Supporting Information Fig. 3A). Analysis of the BMP responsiveness of human native progenitor cells showed that ALK2, ALK3, ACVR2, and BMPR2 (but not ALK6) transcripts were identified in CD45<sup>-</sup>/CD34<sup>+</sup>/CD31<sup>-</sup> cells (Fig. 4B). BMP7 stimulation of progenitor cells induced the phosphorylation of the SMAD1/5/8 complex and P38MAPK but not ERK1/2 (Fig. 4C). When cells were cultured in basal adipogenic media after a 2-day treatment with BMP7 (Fig. 4D), a modest but significant increase of MSCA1-related AP activity and expression (Fig. 4E), a slight but significant increase in triglyceride accumulation (Fig. 4F) and UCP1 protein were observed (Fig. 4G, 4I). The expression of classic adipogenic-related genes (PPAR $\gamma$ 2, ChREBP, GPDH, LPL, and PLIN1) and brite-related genes (UCP1, CITED1, and ELOVL3) was increased in BMP7 pretreated progenitor cells compared to untreated cells (Fig. 4H). Cotreatment with a pharmacological inhibitor of P38MAPK activity (SB203580) led to a decrease in lipid accumulation (Supporting Information Fig. 3E, 3F) and MSCA1-related AP activity (Fig. 4E), while cotreatment with the ERK1/2 pharmacological inhibitor PD98059 had no effect (Supporting Information Fig. 3E, 3F).



About Sections

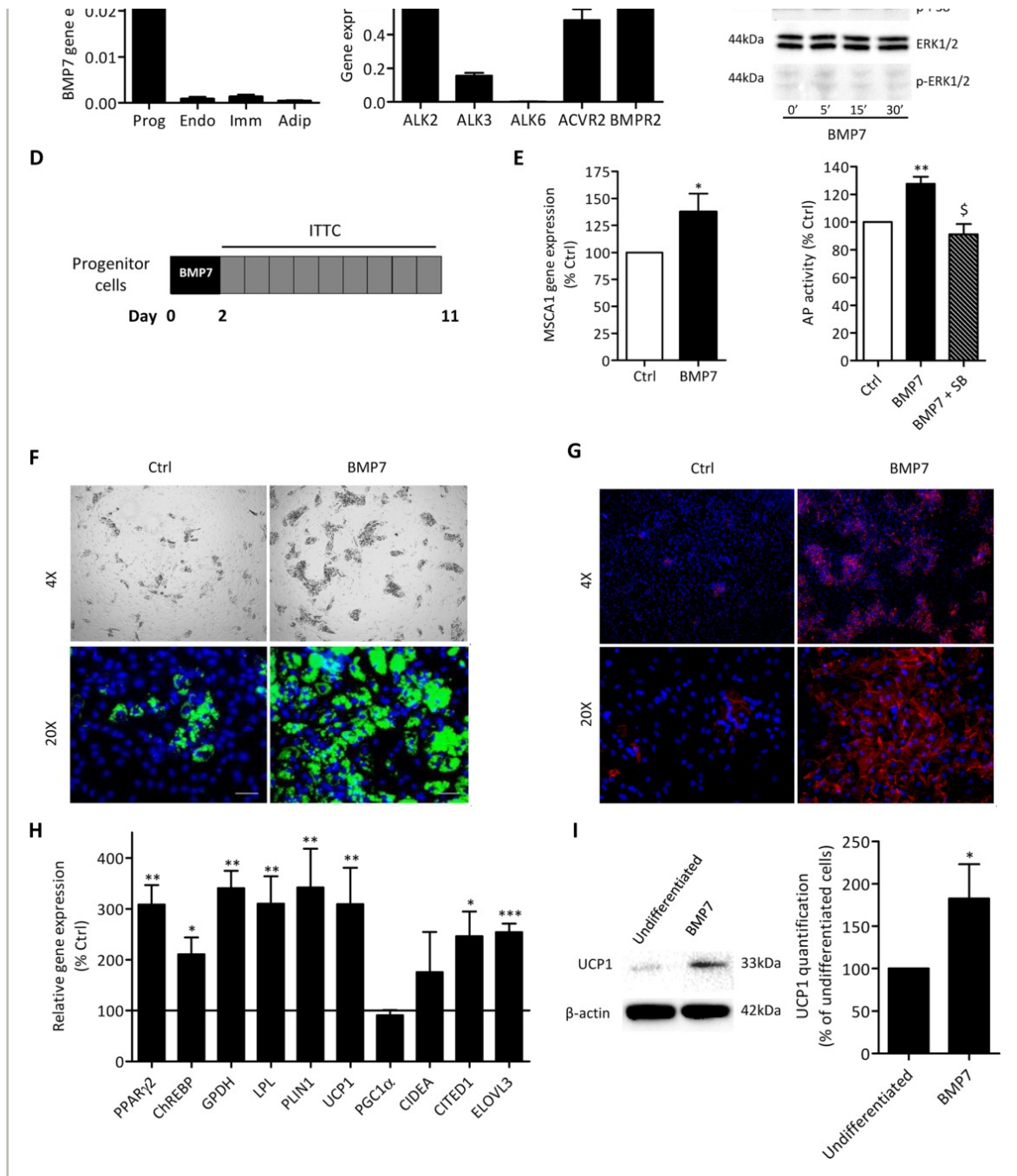


**Figure 4**

[Open in figure viewer](#) | [PowerPoint](#)

BMP7 is locally expressed by progenitor cells and increases MSCA1 expression and activity. **(A)**: BMP7 gene expression in native isolated AT cell populations: CD45<sup>-</sup>/CD34<sup>+</sup>/CD31<sup>-</sup> progenitor cells (Prog), endothelial cells (Endo), immune



 About  Sections



suggesting that MSCA1-related AP activity was involved in brite adipogenesis. CD45<sup>-</sup>/CD34<sup>+</sup>/CD31<sup>-</sup> were transfected with esiRNA against MSCA1 or control and cultured under adipogenic condition containing rosiglitazone for the 3 first days. Reduced MSCA1 gene expression with esiRNA (Fig. 5C) was associated with reduced expression of classic adipogenic-related and brite adipocyte-related genes at day 10 (Fig. 5D). While our data showed that esiRNA treatment resulted in a modest reduction in the levels of MSCA1 transcript, this was in agreement with the range of esiRNA efficiency that can be obtained with native progenitor cells [22](#). We confirmed a functional role for MSCA1 in brite adipogenesis by treating human native progenitor cells with the pharmacological AP inhibitor, tetramisole [23](#). Since the IC<sub>50</sub> of tetramisole on AP activity was described to be around 60 μM [24](#), progenitor cells were treated with 50 μM or 500 μM of tetramisole during rosiglitazone-induced adipogenesis. Lack of toxicity was demonstrated by no changes in cell number (Supporting Information Fig. 4A) and nuclei morphology (data not shown). Inhibition of AP activity by tetramisole led to a concentration-dependent decrease in lipid accumulation (Supporting Information Figure 4B) and expression of classic adipogenic-related and brite adipocyte-related genes at day 10 (PPARγ2, ChREBP, GPDH, LPL, PLIN1, UCP1, CIDEA, CITED1) (Fig. 5E). To note, expression of PGC1α was not modulated.



About Sections

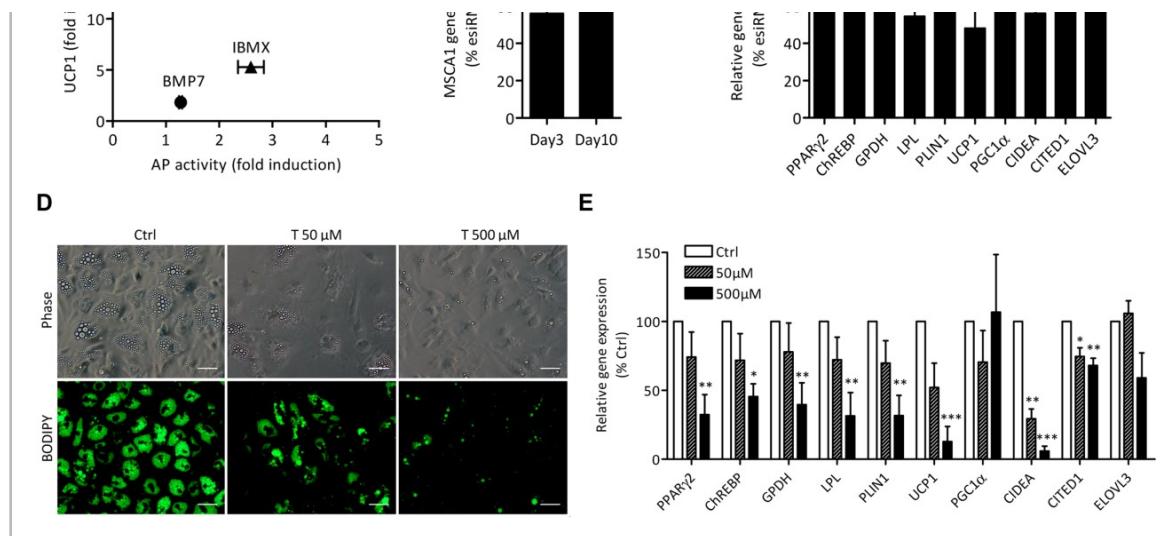


**Figure 5**

[Open in figure viewer](#) | [PowerPoint](#)

MSCA1 activity is involved in white and brite adipogenesis. **(A)**: Association between the level of induction of UCP1 protein at day 10 and MSCA1 AP activity (mean  $\pm$  SEM) after treatment with BMP7 ( $n = 5$ ), IBMX ( $n = 6$ ), or rosiglitazone ( $n = 6$ ). CD45<sup>-</sup>/CD34<sup>+</sup>/CD31<sup>-</sup> progenitor cells were transfected with control esiRNA or esiRNA against MSCA1 and cultured under adipogenic conditions for 10 days with an initial 3 day treatment with rosiglitazone. **(B)**: Relative MSCA1 gene expression at day 3 and day 10 ( $n = 5$ , mean percentage  $\pm$  SEM vs. control cells, \*,  $p < 0.05$ ; \*\*,  $p < .01$ ). **(C)**: Relative expression of indicated genes at day 10 ( $n = 5$ , mean percentage  $\pm$  SEM vs. control cells, \*,  $p < 0.05$ ; \*\*,  $p < 0.01$ ). **(D)**: Representative microphotographs of BODIPY staining of progenitor cells after 10 days of adipogenic culture conditions with rosiglitazone and treated (or not, control, Ctrl) with increasing concentrations of tetramisole (T, 50–500  $\mu\text{mol/L}$ , scale bar = 50  $\mu\text{m}$ ,  $\times 20$  objective). **(E)**: Relative expression of indicated genes in progenitor cells at day 10 treated with increasing concentrations of tetramisole (Ctrl white, 50  $\mu\text{M}$  hatched, 500  $\mu\text{M}$  black) ( $n = 3$ , mean percentage  $\pm$  SEM vs. Ctrl, \*,  $p < .05$ ; \*\*,  $p < .01$ ; \*\*\*,  $p < 0.001$ ). Abbreviations: AP, alkaline phosphatase; BMP7, bone morphogenic protein 7; esiRNA, endoribonuclease-prepared siRNAs; IBMX, isobutylmethylxanthine; T, tetramisole.

Caution ..





About Sections



controlled by gene expression and flow cytometry analyses (Supporting Information Fig. 5A, 5B). Native immunoselected Msca1<sup>+</sup> cells exhibited higher gene expression levels for brite-related genes (CD137, TMEM26, CITED1, CIDEA, ELOVL3), for classic adipogenic-related gene (PPAR $\gamma$ 2, ChREBP, and PLIN1) (Fig. 6A) and a higher mitochondrial content (Fig. 6B) compared to the other two progenitor subsets.  $\beta$ 2-Adrenergic receptor gene expression was higher in Msca1<sup>+</sup> cells compared to other progenitor subsets and to note  $\beta$ 3-adrenergic receptor gene expression was not detected in any progenitor subsets (Fig. 6A). Moreover, PDGFR $\alpha$ , PDGFR $\beta$ , DECORIN, and ZFP423 that were recently described to be expressed by murine preadipocytes were detected but not discriminant between the three human progenitor subsets (Fig. 6A; Supporting Information Fig. 5C). BMP receptors gene expression was found to be equivalent in the three progenitor subsets (Supporting Information Fig. 3D). To note, among the progenitor cell subsets, the  $-/-$  cell subset exhibited the highest levels of BMP7 transcript and propeptide (Supporting Information Fig. 3B, 3C). Hierarchical analysis of differential gene expression between cell subsets clearly highlighted Msca1<sup>+</sup> cells as the progenitor cell subset expressing at the highest level the brite adipocyte-related genes (CIDEA, PGC1 $\alpha$ ,  $\beta$ 2-AR, CD137, ELOVL3, CITED1, PRDM16) and at the lowest level the anti-adipogenic-related genes (KLF2, DNER, or SFRP4) (Supporting Information Fig. 5C). Finally, the adipogenic potentials of the three immunoselected progenitor subsets were analyzed in vitro. Native cells were plated at high density and cultured under ITTCX (brite induction) (Fig. 6C–6H) and ITTCR (white and brite induction) (Fig. 6I–6N). In ITTCX condition, the brite adipogenic potential was clearly supported by Msca1<sup>+</sup> cells as shown by triglyceride accumulation (Fig. 6F, 6E), brite-related gene expression (Fig. 6H), and increased MSCA1 AP activity (Fig. 6D). In ITTCR condition, the three subsets exhibited white and brite adipogenic potential as shown by triglyceride accumulation (Fig. 6L, 6K), brite-related gene expression (Fig. 6N), and UCP1 expression (Fig. 6M; Supporting Information Fig. 7B, 7C) but more marked for Msca1<sup>+</sup> cells. Interestingly, ITTCR condition led to an increase in MSCA1 AP activity and expression in both  $-/Cd271^+$  and  $-/-$  cells (Fig. 6J; Supporting Information Fig. 6C). In depth analyses showed that the  $-/-$  and  $-/Cd271^+$  exhibited hallmarks of less differentiated cells including delay in triglyceride accumulation and a decrease in adipogenic gene expression at day 3 (Supporting Information Fig. 6A, 6B) and smaller lipid droplets (Supporting Information Fig. 7E). To note, we confirm these results using a fluorescence activated cell sorter approach to isolate progenitor cell subsets and validated that magnetic immunoselection/depletion did not affect adipogenic differentiation (Supporting Information Fig. 8).



About Sections

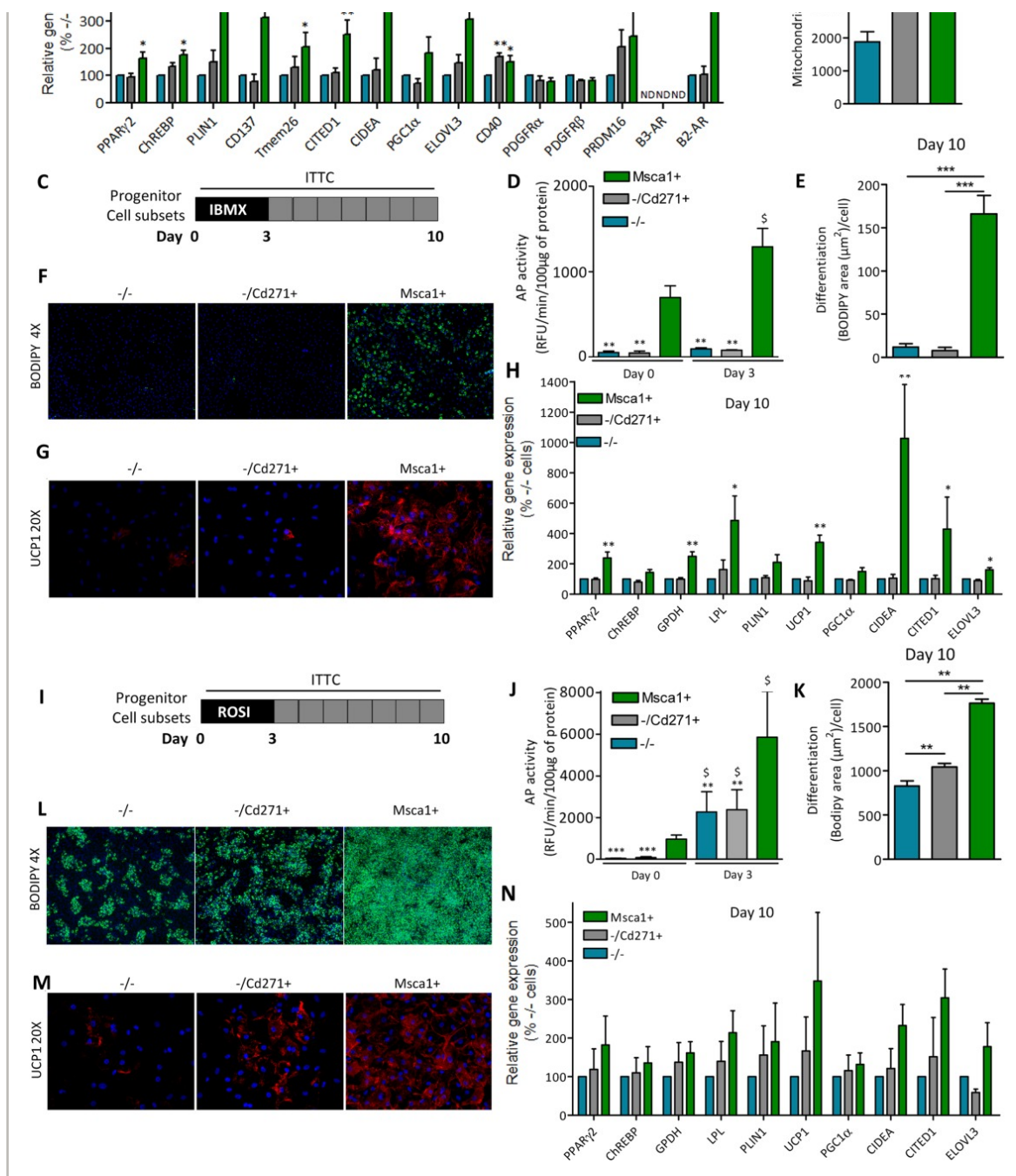


**Figure 6**

[Open in figure viewer](#) | [PowerPoint](#)

Native isolated MscA1+ progenitor subset exhibits brite adipocyte precursor phenotype. **(A)**: Expression of indicated genes in native immunoselected progenitor subsets ( $n=9-10$ , mean percentage  $\pm$  SEM vs.  $-/-$  subset, \*,  $p < .05$ ;



 About  Sections



correlated with BMI (Fig. 7A). MSCA1 gene expression in progenitor cells also increased with obesity (Fig. 7B). Using cohort 2 composed of nonobese ( $\text{BMI} \leq 28 \text{ kg/m}^2$ , Supporting Information Table 2) and morbidly obese women ( $\text{BMI} > 35 \text{ kg/m}^2$ , Supporting Information Table 3), we confirmed that  $\text{Msca1}^+$  cell content in sAT was higher in obese compared to nonobese women (Fig. 7C). In the same cohort, the content of immune cells (including macrophages and T-lymphocytes) was as expected markedly higher in obese compared to nonobese women (Fig. 7C).



About Sections

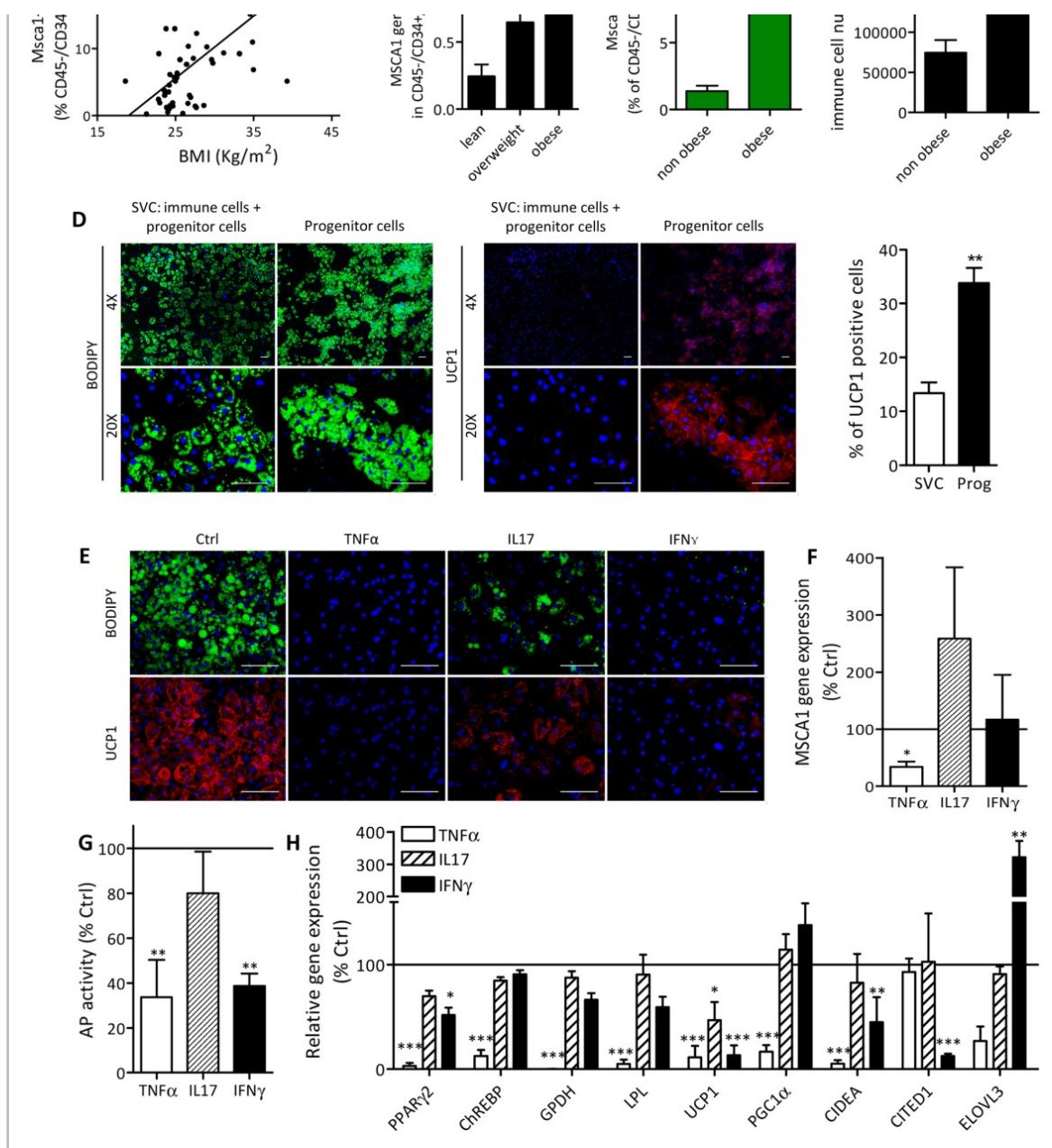


**Figure 7**

[Open in figure viewer](#) | [PowerPoint](#)

Local inflammation inhibits MSCA1 activity and impairs brite adipogenesis. **(A)**: Correlation between BMI (kg/m<sup>2</sup>) and MscA1+ cells percentage in progenitor cells from cohort 1 determined by flow cytometry ( $n = 55$ , Spearman correlation test,  $r = 0.66$ ,  $***$ ,  $p < .001$ ). **(B)**: MSCA1 gene expression in progenitor cells isolated from cohort 1 composed of lean (BMI  $< 25$  kg/m<sup>2</sup>,  $n =$



About Sections



assessed by flow cytometry and immunofluorescence analysis (supporting information 9). To mimic the effect of the presence of immune cells in SVC, progenitor cells were treated with the inflammatory cytokines TNF $\alpha$ , IL17, or IFN $\gamma$ . TNF $\alpha$  and IFN $\gamma$  dramatically reduced lip accumulation and UCP1 expression while IL17 had a modest effect (Fig. 7E). Both TNF $\alpha$  and IFN $\gamma$  markedly inhibited MSCA1 AP activity (Fig. 7G), while only TNF $\alpha$  reduced MSCA1 gene expression (Fig. 7F). In agreement with the involvement of MSCA1 AP activity in brite adipogenesis, both cytokines inhibited the induction of most of the brite adipocyte-related genes (Fig. 7H).

## Discussion

Despite the fact that brite adipocytes are considered to be a therapeutic target of interest in the fight against obesity-related pathologies 25, 26, their existence in human sAT has not been clearly demonstrated. This study, performed on isolated human native progenitor cells, identifies committed progenitor cells with white and brite adipogenic potential as CD45 $^-$ /CD34 $^+$ /CD31 $^-$ /CD271 $^+$ /MSCA1 $^+$ . In situ, Msca1 $^+$  cells exhibit characteristics of the brite precursor phenotype such as high mitochondrial content, elevated expression levels of brite related genes and predominantly located within sAT. Using pharmacological treatments (IBX or rosiglitazone) or an endogenous adipogenic inducer (BMP7), we demonstrate that MSCA1 AP activity is associated with and necessary for adipogenesis, since its inhibition leads to a decrease in the adipogenic potential of human progenitor cells. We demonstrate that Msca1 $^+$  cell content increases with obesity, using two different human cohorts. It is therefore tempting to speculate that the accumulation of Msca1 $^+$  white/brite precursors in sAT with obesity may reveal a blockade of their final differentiation by immune cells, suggesting that local inflammation could contribute to metabolic disorders through an impairment of white/brite adipogenesis.

To identify human native brite precursors within CD45 $^-$ /CD34 $^+$ /CD31 $^-$  progenitor cells, we investigated the expression of additional cell surface markers, namely MSCA1 and CD271. In human bone marrow, both are expressed on progenitor cells that possess adipogenic potential 19, 20. Moreover, AP deficient mice do not possess fat depots 27 and CD271-deficient mice exhibit reduced body weight 28, observations in agreement with a potential involvement of both MSCA1 and CD271 in AT development. Unfortunately, AP deficient mice die a few days after birth 29 and CD271 deficient mice present an elevated neonatal mortality 30. However, no data are currently available concerning their relevance in human AT and/or



About Sections



and exhibited a significantly higher content in human SAT compared to matched white. This location-dependent pattern raised our interest due to the fact that the brite adipogenic potential has been predominantly found in mice SAT [3](#), [12](#), [31](#), [32](#). To assess in vitro adipogenesis, we set up serum-free culture conditions that use a short-term inducer treatment followed by culture in minimal adipogenic media. This protocol was designed to exclude chronic inducer effects on gene expression and focus on the differentiation state. Induction of white/brite adipogenesis by rosiglitazone treatment has been already reported in mice as well as in human multipotent adipose derived stem cells [5](#), [7](#), [17](#), [33](#) and in vivo long term PPAR $\gamma$  agonist administration was reported to promote the appearance of brite adipocytes in mice [6](#). In this study, we demonstrated that short-term rosiglitazone induced brite adipogenesis in human native progenitor cells. Moreover mitochondrial changes were observed, with an increase in expression of proteins responsible for oxidative phosphorylation, and a morphological transformation from an elongated to a fragmented network, a hallmark of mitochondrial activation in rodent brown AT [34](#). Induction of white/brite adipogenesis by rosiglitazone was associated with a rapid upregulation of the MSCA1 transcript and AP activity prior to lipid accumulation. Furthermore, approaches using either esiRNA against MSCA1 or pharmacological inhibition of AP activity led to a decrease in white and brite adipogenesis, demonstrating a functional involvement of MSCA1 in the adipogenic processes.

Catecholamines such as norepinephrine have been described to promote brite adipogenesis in rodent models through  $\beta$ 3-adrenergic stimulation and a subsequent increase in intracellular cAMP [8](#), [32](#). Differences in expression of  $\beta$ -adrenergic receptors in AT were documented between rodent and humans [2](#) and no  $\beta$ 3-adrenergic receptor activity was found in human [35](#), [36](#). Since the native human progenitor subsets do not express  $\beta$ 3-adrenergic receptor, we tested the impact of IBMX, an inhibitor of phosphodiesterases that increases intracellular cAMP. We found that IBMX was not only able to specifically induce brite-related genes but also an increase both the expression and activity of MSCA1, albeit this induction was less pronounced than with rosiglitazone treatment. Finally, we investigated the involvement of a physiologically relevant brite inducer, BMP7, reported to play a major role in brown AT development in mice and to promote differentiation of murine brown preadipocytes [10](#), [37](#). Short-term BMP7 treatment led to white and brite differentiation and increased MSCA1 expression and activity in human progenitor cells. The extent of brite differentiation obtained after our 2 day treatment with BMP7, while modest compared to our other cell culture conditions, is in agreement with a recent publication reporting a brite adipogenic induction after a 14 day



About Sections



...interconversion, suggesting that brite-mediated upregulation of MSCA1 activity requires P38MAPK. In rodents, activation of P38MAPK has been shown to be involved in brite adipogenesis induced by both the  $\beta$ 3-adrenergic receptor as well as PPAR $\gamma$  agonists [39](#). Moreover, P38MAPK has been described to enhance stability of PGC1 $\alpha$  and to promote uncoupled respiration in muscle cell mitochondria [40](#). It is thus tempting to speculate that P38MAPK could be at the crossroads of the pathways activated by the various brite inducers. Future experiments will focus on defining the role of P38MAPK in brite adipogenesis.

In mice, the origin of brite adipocytes remains under debate. Some studies showed white to brite adipocyte conversion [11](#) while others highlighted the differentiation of specific precursors into brite adipocytes in mice [12](#), [13](#) and in a human cell line [41](#). Although we can exclude the existence of mechanisms that allow human white to brite adipocyte interconversion, we identify MSCA1 as a functional marker of human native white and brite precursor cells. Indeed, *in situ*, *MscA1*<sup>+</sup> cells exhibited a brite precursor cell phenotype with high mitochondrial content and elevated expression levels of brite precursor-related genes including CD137, TMEM26, CIDEA, CITED1, and ELOVL3 [4](#). To note, CD40, a rodent brite-related marker [4](#), did not allow a clear segregation between the distinct human progenitor cell subsets, suggesting additional species-specific differences. PDGFR $\alpha$  [13](#), PDGFR $\beta$  [42](#), [43](#), and DECORIN [44](#), described as markers of white adipose progenitors either in rodent or human were detected at similar levels in the three progenitor subsets. The study of Berry et al. highlighted that the rodent PDGFR $\alpha$  cells were composed of two cell subsets at distinct stages of white adipogenic process, preadipocytes being defined by lack of CD24 expression [45](#). In human white adipose tissue (WAT), no cell surface markers are available to discriminate the progenitor cells according to adipogenic state [46](#), stressing further the need for relevant positive markers for preadipocytes. Our study identifies MSCA1 as a positive functional marker of the human preadipocyte. Lack of MSCA1 in *-/Cd271*<sup>+</sup> and *-/-* subsets emphasizes their immature state toward the adipogenic program. Indeed, under rosiglitazone culture conditions both *-/Cd271*<sup>+</sup> and *-/-* subsets exhibited a delayed adipogenic potential, associated with the induction of MSCA1 gene expression and AP activity, indicating that the *MscA1*<sup>+</sup> subset may arise from both subsets.

Finally, by the use of two independent cohorts, we show that the *MscA1*<sup>+</sup> cell content is high in sAT from obese compared to nonobese women. We speculated that such an increase may originate from accumulation of *MscA1*<sup>+</sup> precursor cells that do not undergo further differentiation. To analyze the local signals that could block differentiation, we investigated t



About Sections



...s, specifically test their brite adipogenic potential. We focused our search on three candidate inflammatory cytokines already described to inhibit adipogenesis but that have not been studied in the context of brite adipogenesis, TNF $\alpha$  47, 48, IFN $\gamma$  49, and IL17 50. IFN $\gamma$  and IL17 did not affect MSCA1 gene expression but all three cytokines inhibited MSCA1 activity and subsequent brite adipogenesis, albeit to varying degrees. In murine models, anti-inflammatory macrophages have been shown to promote appearance of brite adipocytes whereas proinflammatory macrophages do not 51-54. Recent studies performed in mice showed that impaired brite adipogenic potential is associated with metabolic dysfunctions such as type 2 diabetes 31, 32, 55. The involvement of an immune component in the impairment of brite adipogenesis represents an intriguing mechanism. We hypothesize that immune cell infiltration within AT occurring with obesity, if persistent, will create a deleterious inflammatory microenvironment that could disrupt the dynamic turn-over of adipocytes in human SAT leading to the accumulation of Msca1+ precursor cells blocked in a nondifferentiated state.

## Conclusion

We have demonstrated the existence of a common white and brite-competent progenitor cell subset within human AT characterized as CD45 $^{-}$ /CD34 $^{+}$ /CD31 $^{-}$ /CD271 $^{+}$ /MSCA1 $^{+}$ . In addition, we have shown that MSCA1 plays a functional role in white and brite adipogenesis which is impaired by immune cells. Therefore, we reveal multiple avenues for therapeutic intervention against metabolic diseases. First, anti-inflammatory strategies could ameliorate the metabolism of obese individuals by improving AT expandability and/or brite adipogenesis. Second, the AP activity of MSCA1, or downstream effectors, could be targeted to improve adipogenesis directly.

## Acknowledgments

This work was financially supported by the INSERM, Sanofi-Aventis R&D, Clarins Dermocosmetique, and the region Midi-Pyrénées. We acknowledge Grolleau-Raoux from aesthetic surgery department, Rangueil Hospital, and Doctor N'Guyen from gynecology-obstetrics department, Louis Mourier Hospital, for the collection of AT samples and their associated patient information. We appreciate greatly the advice from the Cellular Imaging facility TRI platform and GeT-TQ transcriptomic platform.

## Author Contributions





 About  Sections



and final data analysis and interpretation, from data analysis and interpretation and manuscript writing; A.R.: conception and design; P.F.: conception and design and data analysis and interpretation; M.L.: conception and design; A.B.: conception and design, data analysis and interpretation, manuscript writing, and final approval of manuscript. D.E. and N.B. contributed equally to this work.

## Disclosure of Potential Conflicts of Interest

The authors indicate no potential conflicts of interests.

Supporting Information 

References 

Citing Literature 



© 2018 AlphaMed Press  
STEM CELLS  
STEM CELLS Translational Medicine  
The Oncologist



 About  Sections



**About Wiley Online Library**

**Help & Support**

**Opportunities**

**Connect with Wiley**

Copyright © 1999-2018 John Wiley & Sons, Inc. All rights reserved





 About     Sections

